ELSEVIER

Harvesting energy from the marine sediment–water interface II Kinetic activity of anode materials[☆]

Daniel A. Lowy [a,*], Leonard M. Tender [b,**],
J. Gregory Zeikus [c], Doo Hyun Park [d], Derek R. Lovley [e]

[a] *Nova Research, Inc., 1900 Elkin St., Alexandria, VA 22308, United States*
[b] *Center for Bio/Molecular Science and Engineering-Code 6900, Naval Research Laboratory, Washington, DC 20375, United States*
[c] *Department of Microbiology and Molecular Genetics, Michigan State University, East Lansing, MI 48824, United States*
[d] *Department of Biological Engineering, Seokyeong University, Seoul 136-704, Republic of Korea*
[e] *Department of Microbiology, Univeristy of Massachusetts, Amherst, MA 01003, United States*

Abstract

Here, we report a comparative study on the kinetic activity of various anodes of a recently described microbial fuel cell consisting of an anode imbedded in marine sediment and a cathode in overlying seawater. Using plain graphite anodes, it was demonstrated that a significant portion of the anodic current results from oxidation of sediment organic matter catalyzed by microorganisms colonizing the anode and capable of directly reducing the anode without added exogenous electron-transfer mediators. Here, graphite anodes incorporating microbial oxidants are evaluated in the laboratory relative to plain graphite with the goal of increasing power density by increasing current density. Anodes evaluated include graphite modified by adsorption of anthraquinone-1,6-disulfonic acid (AQDS) or 1,4-naphthoquinone (NQ), a graphite-ceramic composite containing Mn^{2+} and Ni^{2+}, and graphite modified with a graphite paste containing Fe_3O_4 or Fe_3O_4 and Ni^{2+}. It was found that these anodes possess between 1.5- and 2.2-fold greater kinetic activity than plain graphite. Fuel cells were deployed in a coastal site near Tuckerton, NJ (USA) that utilized two of these anodes. These fuel cells generated ca. 5-fold greater current density than a previously characterized fuel cell equipped with a plain graphite anode, and operated at the same site.
© 2006 Elsevier B.V. All rights reserved.

Keywords: Microbial fuel cell; Magnetite; Tafel plots; Kinetic activity; Power density

1. Introduction

Recently a microbial fuel cell was demonstrated, at two coastal marine sites, that is being developed to operate low-power consuming marine deployed scientific instrumentation (Fig. 1) (Tender et al., 2002). This fuel cell consists of a graphite plate anode buried in marine sediment connected by an external circuit to a graphite plate cathode positioned in overlying seawater. Open circuit cell voltage is typically 0.75 ± 0.03 V. Maximum power density is typically 10–20 mW/(m² geometric area of the anode), depending on the discharge potential and geochemical characteristics of the site (Tender et al., 2002). Such a fuel cell generates power by oxidizing sediment organic matter with seawater oxygen. It does so by utilizing a naturally occurring redox gradient that spans oxidant-rich seawater and reductant-rich sediment millimeters to centimeters beneath the sediment surface (Tender et al., 2002; Reimers et al., 2001). The redox gradient results from microbial activity in marine sediment; it is a common feature of the seafloor of continental margins and the source of the fuel cell voltage (Froelich et al., 1979). Cathodic current is attributed to reduction of seawater oxygen owing to similarity of the cathode to that of seawater batteries (Wilcock and Kauffman, 1997). Anodic current is a result of two types of concurrent reactions: (i) oxidation of sediment reductants and (ii) reduction of the anode by microorganisms that colonize the anode. Sediment of continental margins is often
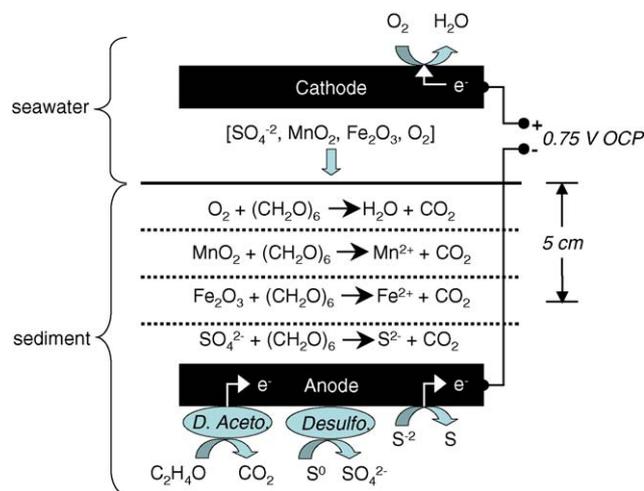

Fig. 1. Schematic representation of the operating principle of the mediator less sea floor microbial bio-fuel cell (based on refs: Avila et al., 2000; Bard and Faulkner, 2001; Bond et al., 2002). See explanations in text.

rich in organic matter. Microbial oxidation of this organic matter is limited by flux of oxidants from overlying seawater (listed in Fig. 1 below the cathode in order of increasing oxidation potential). Sediment dwelling microorganisms therefore utilize a depth dependent succession of oxidants in order of decreasing oxidation potential with increasing sediment depth, given that less potent oxidants liberate less energy per equivalent organic matter oxidized (represented in Fig. 1 as glucose) (Reimers et al., 2001).

Fig. 1 illustrates the operating principle of the mediator less sea floor microbial bio-fuel cell. In the generalized case illustrated here, microbes in the sediment surface layer preferentially reduce O_2 in oxidation of organic matter, leaving MnO_2, Fe_2O_3, and SO_4^{2-} unutilized. MnO_2 is then microbially reduced in the next lowest sediment layer, Fe_2O_3 in the third sediment layer, and SO_4^{2-} in the forth sediment layer. As a consequence, each layer accumulates more potent reductants (Mn^{2+}, Fe^{2+}, and S^{2-}) with increasing sediment depth. This reductant gradient generates the open circuit voltage of the fuel cell, and renders the sediment imbedded electrode the anode and the seawater electrode the cathode. At least three reactions have been determined to occur at the anode: (1) oxidation of S^{2-} to S^0; the importance of dissolved and solid state sulfides as electron donors in anoxic marine sediments has been recently emphasized (Reimers et al., 2005), and the amplification of the biogeochemical cycle of sulfur and iron by the fuel cell deployed in the Yaquina Bay estuary discussed (Ryckelynck et al., 2005); (2) microorganisms colonizing the anode in the family Geobacteracea (most similar to *Desulfuromonas acetoxidans*) oxidize acetate in sediment and directly reduce the anode; (3) microorganisms colonizing the anode most similar to species in the *Desulfobulbus* or *Desulfucapsa* genera oxidize anode generated S^0 to SO_4^{2-}. The enrichment of anodic biofilms in *Desulfobulbus* or *Desulfucapsa* genera was reported by Lovley et al. (Holmes et al., 2004a,b). These microorganisms may mediate electron transfer by either direct bacterial transfer, i.e., without addition of exogenous elec-

tron transfer mediators (Tender et al., 2002; Bond et al., 2002) (e.g., in the case of Geobacteracea) (Bond and Lovley, 2003) or by excretion of redox components (Mahadevan et al., 2006). Sustained current is attributed to continual replenishment of electrode reactants by diffusion (anode and cathode) and seawater flow (cathode) (Bond et al., 2002). A fuel cell operating at one of the deployment sites for the past ~1.5 years continuously sustains approximately $30\,mW\,m^{-2}$ ($90\,mA\,m^{-2}$) at a cell voltage of 0.3 V, with no indication of exhaustion. Kinetic activity of the anode, which limits overall power current density (and thus power generation), was determined by separate measurement of anode and cathode overpotentials (Reimers and Tender, 2002).

In order to increase the current density and, as a result, the power density of fuel cells of this design, we focused attention on enhancing the kinetics of microbial reduction of the anode. Specifically, graphite anodes modified with or incorporating known microbial oxidants where evaluated in comparison to plain graphite. A kinetic activity (KA) for each type of anode is therefore reported. KA was determined by normalization of the average i_0 for each anode type by i_0 of a plain graphite anode determined in a cell of the same configuration. Our described research is justified by the observation that all anodes evaluated here demonstrated greater KA than graphite (considered, by convention, equal to 1.0). The KA of graphite–ceramic composite anodes containing Mn^{2+} and Ni^{2+} was 2.2 (highest) and for AQDS-modified graphite anode was 1.7. Fuel cells deployed in a previously utilized coastal site near Tuckerton, NJ, USA (Tender et al., 2002; Reimers et al., 2001) utilizing these anode materials generated, before onset of mass-transfer limitation, ~5-fold greater current density than a fuel cell equipped with a plain graphite anode.

2. Experimental

2.1. Anode preparation

2.1.1. Anodes modified with AQDS and NQ

For the laboratory evaluation, graphite disks (9.53-cm diameter, 1.27-cm thick, LG grade 10, Graphite Engineering and Sales, Greenville, MI, USA) were lightly sanded, rinsed with dionized water (DIW), then modified with anthraquinone-1,6-disulfonic acid (AQDS) by immersion in $50\,mmol\,L^{-1}$ AQDS (>97%, purity, Fluka Chemika, Buchs, Switzerland, used as received) in $0.1\,mol\,L^{-1}$ perchloric acid (prepared from 70% $HClO_4$, A.C.S. reagent grade, Aldrich, used as received) for 48 h, at room temperature. The concentration of the AQDS solution was set by the solubility of the quinone in perchloric acid, while the duration of immersion was optimized by colorimetric monitoring. These electrodes were then rinsed with copious amounts of DIW (18.2 Mohm cm, Milli-Q Synthesis System, Milipore). In a similar fashion, graphite disk electrodes were modified with 1,4-naphthoquinone (NQ) by soaking in $63\,mmol\,L^{-1}$ NQ in ethanol (200 proof, 95.5% purity, A.C.S. reagent grade, Aldrich, used as received), for 72 h. A water insulating oceanographic bulk head connector and matching 18-AWG cable (Impulse Enterprise, San Diego, CA, USA) was used as previously described

(Tender et al., 2002; Bond et al., 2002) for electrical connection to each electrode. The AQDS modified graphite anode of the deployed fuel cell was prepared in the same manner as above using a 48.3-cm diameter, 1.27-cm thick graphite disk disks.

2.1.2. Ceramic–graphite composite anodes containing Mn^{2+} and Ni^{2+}

Preparation of these anodes was previously described (Park and Zeikus, 2002, 2003). Briefly, they were obtained by mixing 3 wt.% $MnSO_4·H_2O$ and 1.0 wt.% $NiCl_2·6H_2O$ to a 2:1 (w/w) mixture of fine graphite powder (particle size below 500 mesh) and inorganic binder (kaolin with particle size below 400 mesh). Two parts of this mixture were stirred into a paste with one part DIW and molded into a 24.8 cm diameter, 1.43 cm thick disk by pressing at 1 kg cm^{-2} and drying in air for 24–48 h at room temperature, then solidified by baking in a kiln at 1100 °C for 12 h under inert atmosphere (N$_2$ gas). For the laboratory testing, 7.1 cm long, 5.1 cm wide, 0.8 cm thick pieces were sawed from each plate and used for evaluation. Electrical contact to each electrode was made as described above. For the deployed fuel cell, an entire disk was used as the anode.

2.1.3. Anodes modified with Fe_3O_4

Nanocrystalline magnetite, Fe_3O_4, was prepared according to the following procedure adapted from that reported by Chen and co-workers (Fan et al., 2001). First, 1.39 g (0.1 mol L^{-1}) of $FeSO_4·7H_2O$ (>99%, Alfa Aesar, Ward Hill, MA) and 0.79 g (0.11 mol L^{-1}) of $Na_2S_2O_3$ (Sigma Chemical Co.) were dissolved in 50 mL DIW. This solution was mixed together with 10 mL (two equivalents) of 1 mol L^{-1} NaOH solution (Sigma Diagnostics, St. Louis, MO) which yielded a black precipitate. The entire mixture was heated in a pressure vessel (Model No. 921 Pressure Cooker, Wisconsin Aluminum Foundry Co., Inc., Manitowoc, WI, total volume 21.5 Qt) and maintained at 122 °C for 24 h, then cooled to room temperature. The resulting dark gray precipitate (microcrystalline Fe_3O_4) was collected by filtration, washed repeatedly with DIW and absolute ethanol, and then dried in vacuum at 70 °C for 4 h. To make the Fe_3O_4 paste modified electrode, 0.30 g (3.0 wt.%) of the Fe_3O_4 was incorporated in a mixture of 6.0 g graphite powder (−325 mesh, 99.999%, Aldrich) and 3.6 g kaolin (finest powder, Riedel-de-Häen, Seelze, Germany), according to previously described procedures (Park and Zeikus, 2002, 2003). Minimum DIW was added to form a slurry, which was applied on the top and bottom of a plain graphite disk electrode (described above), dried at 90 °C for 30 min, then baked at 250 °C for 48 h in air, to yield an ∼3 mm-thick type layer on the electrode top and bottom. Electrical contact was made as described above. To prepare the Fe_3O_4 and nickel paste electrode, the same procedure was followed as above but with the addition of 0.10 g (1.0 wt.%) of $NiCl_2$ incorporated into the mixture of Fe_3O_4, graphite powder, and kaolin.

Plain graphite disc electrodes (described above), lightly sanded and rinsed with DIW, were used as anodes for comparison and as counter electrodes with and without having been soaked in 0.1 mol L^{-1} $HClO_4$ for 48 h, at room temperature with no discernible difference.

2.2. Laboratory electrochemical cells

As previously described, a seawater/sediment interface can be reassembled in the laboratory using harvested sediment and seawater (Reimers et al., 2001). Sediment (collected with a clean shovel and clean PVC bucket) and seawater (collected with a clean Nalgene carboy) utilized here originated from the Rutgers University Marine Field Station, Tuckerton, NJ, USA (39° 30.5′N, 74° 19.6′W). This sediment was previously characterized and no attempt was made to preserve the redox gradient (Tender et al., 2002; Bond et al., 2002). Fig. 2 schematically illustrates the two cell configurations used to measure the kinetic activity of the anodes evaluated.

In both configurations, the anodes were positioned in ∼0.7 L of wet sediment (as collected) added to clean 2-L beakers. Each beaker was then filled to ∼1.9 L with seawater, which unsettled some sediment. Within hours, the sediment re-settled to the bottom of the beaker, hence, the seawater/sediment interface was reassembled (Reimers et al., 2001). A graphite disk counter electrode and an Ag/AgCl, sat. KCl reference electrode (Bioanalytical Systems, Inc., IN) were then positioned in the overlying seawater and an open circuit voltage between the anode and counter electrode (typically ∼0.725 V) was measured.

Fig. 2A illustrates the configuration used to evaluate a single anode per cell. Fig. 2B displays the configuration used for testing three anodes per cell. No procedures were used to maintain these cells with the exception of periodic addition of DIW to compensate evaporation loss. At room temperature, we have found that such cells can maintain an open circuit cell voltage of 0.675–0.750 V for at least 6 months.

2.3. Laboratory electrochemical measurements

Electrochemical measurements were performed in the laboratory using either a Model 283 PAR Potentiostat (Princeton Applied Research) and CoreWare software (Scribner Associates, Inc.) or a Model 660 Electrochemical Workstation (CH
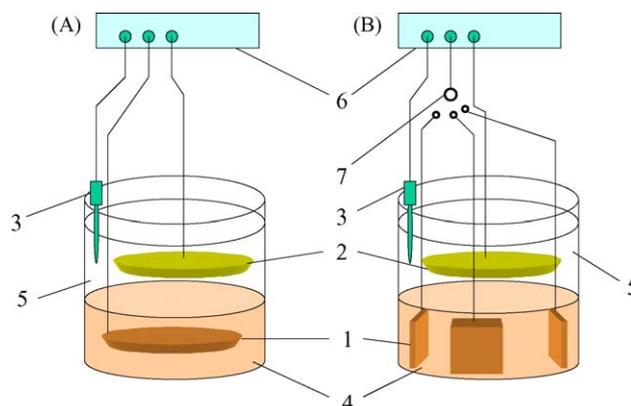

Fig. 2. Schematic of the microbial fuel cells used for recording OCP and Tafel plots: (A) system equipped with disk electrodes, (B) system equipped with three anodes. (1), Anode buried in sediment; (2), Cathode immersed in sea water; (3), Ag/AgCl, sat. KCl reference; (4), Marine sediment; (5), 2 L glass beaker; (6), Electrochemical workstation; (7), Switch for connecting various chemically modified anodes.

Instruments, Austin, TX). For each anode, exchange current density (i_0) was determined from Tafel plots generated in a 2-L laboratory cell. In order to minimize limitations to current density imposed by the cathode, measurements were conducted in a 3-electrode configuration using a reference electrode in seawater, the sediment imbedded anode as the working electrode, and the cathode in seawater as the counter electrode. Multiple Tafel plots (log[current density] versus overpotential, η) were recorded for each anode (working electrode) by sweeping voltage at $1\,mV\,s^{-1}$ from $\eta = 0$–$100\,mV$ (most cases), where $\eta = 0$ is the open circuit potential (OCP) of the anode versus the reference electrode. Non-negligible differences among Tafel plots were recorded for the same type of anode in different cells presumably due to variability in sediment and cell configuration. At least 8 h were required for a stable OCP to re-establish between measurements.

2.4. Measurements of power generation by marine deployed fuel cells

A fuel cell similar to that previously described (Tender et al., 2002), but lacking a container to recover sediment above and below the anode was used to sequentially evaluate a 48.6-cm diameter, 1.27-cm thick AQDS-modified graphite disk anode and a 24.1-cm diameter, 1.27-cm thick graphite–ceramic anode containing $NiCl_2$ and $MnSO_4$. The cathode consisted of a 48.26-cm diameter, 1.27-cm thick graphite disk. A PVC scaffold was used to position the anode $\sim 10\,cm$ below the sediment surface and the cathode $\sim 20\,cm$ above the sediment surface in $\sim 1\,m$ deep water (mean low tide). A Model 870 computer controlled resistive load (Scribner Associates, Inc.) was used to generate polarization plots (i.e., voltage and power density versus current density) for each fuel cell based on the foot print area of the anode (0.183 and $0.457\,m^2$, respectively) (Tender et al., 2002). The resistive load is incorporated within an instrument package that is deployed with the fuel cell (Neptune Sciences, Inc.) and communicates with a shore-based computer.

3. Results and discussion

For each Tafel plot, recorded as described in Section 2, the exchange current density, i_0, was determined in the time honored manner by extrapolation to $\eta = 0$ of a linear regression ($R^2 > 0.99$) between $\eta = 60$–$80\,mV$ (Fig. 3) (Bard and Faulkner, 2001). By choosing this low overpotential range the i_0 values will depend on the charge limited electrochemical process, the effect of mass transfer being negligible.

Table 1 summarizes results of the laboratory evaluation of the five types of graphite-based anodes examined here in comparison to plain graphite. The open circuit potentials (OCP) of NQ-modified and AQDS-modified graphite anodes are similar to, if not indistinguishable from those of plain graphite anodes. This suggests the same electron-transfer reactions proceed at these electrodes. This is consistent with use of AQDS as an oxidant of microorganisms in the family Geobacteracea in solution (Lovley et al., 1996) and with XPS analysis of graphite (albeit
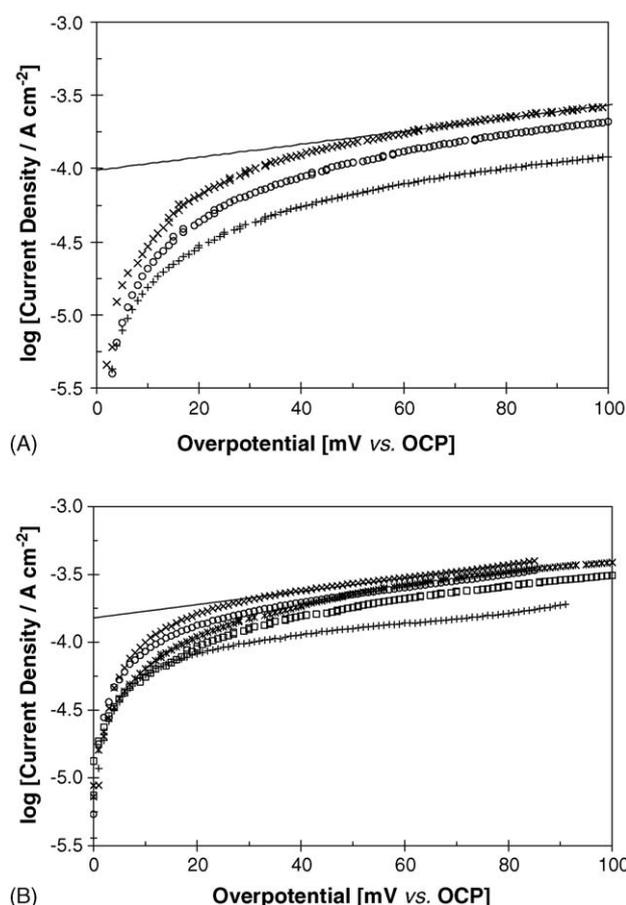

(A)

(B)

Fig. 3. Tafel plots: (A) Tafel plots recorded in a fuel cell equipped with two anodes (Fig. 2A), with graphite anodes previously coated with ceramics layers containing (i) $Mn^{2+} + Ni^{2+}$ metallic graphite ×, (ii) graphite modified with AQDS ◯, relative to a plain graphite anode + (overpotential range: 0–600 mV vs. OCP, scan rate: $1\,mV\,s^{-1}$; reference electrode: Ag/AgCl, sat. KCl, only one linear fir shown). (B) Tafel plots recorded in a fuel cell equipped with three square-shaped anodes (Fig. 2B): graphite disk modified with (i) magnetite: (×), (ii) Ni-magnetite: (◯), (iii) AQDS: (*), (iv) NQ: (□), and (v) plain graphite: (+), used alternatively in conjunction with the same plain graphite disk cathode (same conditions as in Fig. 3A).

from a different source) indicating multiple carbon and oxygen containing functional groups including quinone-like structures exist on plain graphite surfaces (Wu et al., 2002). While the exact mechanisms of microbial reduction of quinone and of graphite are not known, we suspect outer membrane cytochromes are the reducing agents (Lovley et al., 2004).

Electrochemistry of cytochromes immobilized on gold electrodes modified with carboxylic acid-terminated self-assembled monolayers is highly studied (Clark and Bowden, 1997; El Kasmi et al., 1998; Collinson et al., 1992; Tarlov and Bowden, 1991; Avila et al., 2000). Reported results suggest that electrostatic interactions between such electrodes and cytochromes favor orientations of cytochromes in which their heme rings are positioned relatively close to the electrode surface resulting in relatively fast electron-transfer. In a similar fashion, we suspect quinone on graphite electrodes orientate cytochromes in the outer membrane of Geobacteraceae. Enhancement in KA of the quinone-modified anodes (1.5 and 1.7) may therefore

Table 1

Electrocatalytic activity of various chemically modified graphite anodes relative to plain graphite (based on exchange current density and current density values at three overpotential values, obtained from Tafel plots[a])

Anode	Open circuit potential vs. Ag/AgCl (mV)	Kinetic Activity (KA)
Graphite–ceramic containing $Mn^{2+} + Ni^{2+}$	-318 ± 25	2.2
Graphite paste[b] containing Fe_3O_4	-440 ± 4	2.1
Graphite paste[c] containing $Fe_3O_4 + Ni^{2+}$	-472 ± 28	1.7
AQDS-modified graphite[d]	-403 ± 15	1.7
NQ-modified graphite[d]	-411 ± 12	1.5
Graphite[d]	-411 ± 16	1.0

Geometric surface area of the anode (a–c): $71.3\, cm^2$.

[a] Mean values of 5–12 independent experimental runs.

[b] 5 wt.% of microcrystalline Fe_3O_4 in ceramic coatings on the surface of plain graphite; Tafel plot recorded in the overpotential range from 0 to 85 mV.

[c] 5 wt.% of microcrystalline Fe_3O_4 + 1 wt.% $NiCl_2 \cdot 6H_2O$ in ceramic coatings on the surface of plain graphite (all experimental parameters are identical to b).

[d] Experiments conducted under identical conditions, in a cell with three anodes (graphite modified with AQDS, graphite with 1,4-NQ, and plain graphite; geometric surface area: $23.2\, cm^2$) imbedded in the same sediment. The same plain graphite cathode was used throughout the experiments.

reflect higher quinone surface density compared to that of native quinone on graphite.

The OCPs of the iron-containing anodes and manganese-containing electrodes are different from each other and from that of plain graphite anodes, indicating that different electron-transfer reactions occur at each of these anode types. The higher OCP of the iron-containing anodes compared to that of the manganese-containing electrodes is consistent with the higher oxidation potential of Fe-oxide compared to that of manganese dioxide (Froelich et al., 1979) (Fig. 1), and suggests Fe_2O_3 and MnO_2 are being reduced at theses anodes, respectively. The high KA of these anodes (1.7–2.2) is consistent with the known property of microorganisms in the family Geobacteracea to oxidize insoluble iron oxide and manganese oxide in marine sediment (Bond et al., 2002).

Fig. 4 displays typical polarization plots of the deployed fuel cell, first equipped with an AQDS-modified graphite anode, then with a graphite ceramic composite anode containing Mn^{2+} and Ni^{2+}.

Both deployments were conducted with a plain graphite cathode. A similar fuel cell using a plain graphite anode could sus-

tain maximum power of $\sim 20\, mW/m^2$ ($\sim 66\, mA/m^2$) at 0.30 V (Tender et al., 2002). When operated with AQDS-modified anode, the deployed fuel cell reached its maximum power density of $\sim 98\, mW/m^2$ ($\sim 560\, mA/m^2$) at the cell voltage of 0.24 V. When utilizing the Mn^{2+} and Ni^{2+} anode, the deployed fuel cell achieved a maximum power density of $\sim 105\, mW/m^2$ ($\sim 350\, mA/m^2$) at 0.35 V. Over time (several days), while discharging at fixed voltage, the current density for the fuel cell configured with both anodes decreased with square root of time, indicating mass transfer limited current density, and hence, diffusion limited kinetics. By placing the fuel cell in open circuit for a sufficiently long time (ca. 24 h), the maximum current density could be reached repeatedly, indicating that the kinetic enhancement is robust. Fuel cells operated with plain graphite anode have produced sustained power indefinitely, while AQDS-modified electrodes initially produce five-times greater power, then gradually decay over time to the performance of the graphite anode. During long-term experiments the current density for AQDS-modified graphite decreases with the square root of time, which suggests mass transfer limitation. Upon interruption of the operation of the fuel cell, the anodic area replenishes with "fuel", and the current density returns to the initial high value. Our ongoing work addresses the mass transfer limitations. Deployment of the kinetically enhanced fuel cells in environments with higher concentrations of anode reactants (such as methane/sulfide vents) would enable sustained power generation of $\sim 100\, mW/m^2$.

4. Conclusion

As it is stable over extended time periods (experiments have been conducted up to 18 months), the explored microbial bio-fuel cell is a promising sustained power source for many low-power marine-deployed instruments, including seismic detectors and monitoring devices. In order to increase the power density of such fuel cells several electrode modification strategies and techniques have been researched. Anode materials modified with inorganic or organic charge transfer mediators have proven kinetically advantageous over plain graphite. Our current work addresses mass transfer limitations by alternative techniques.
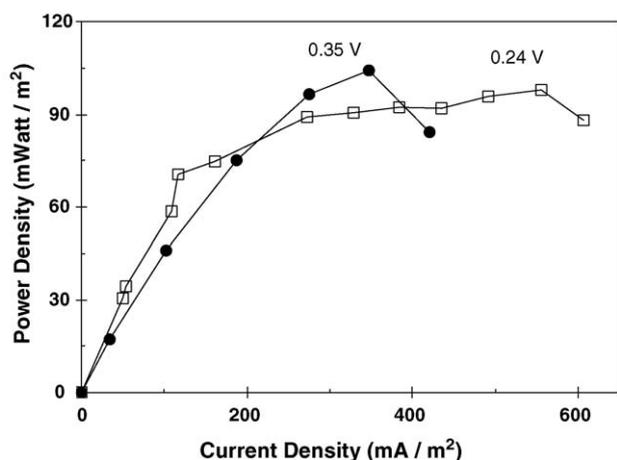

Fig. 4. Power density vs. current density curves for a fuel cell operated in Tuckerton, NJ utilizing first an AQDS-modified anode (□) and then a graphite ceramic anode containing Mn^{2+} and Ni^{2+} (●). Voltage at maximum achieved power indicated.

Acknowledgements

References

Avila, A., Gregory, B.W., Niki, K., Cotton, T.M., 2000. An electrochemical approach to investigate gated electron transfer using a physiological model system: cytochrome c immobilized on carboxylic acid-terminated alkanethiol self-assembled monolayers on gold electrodes. J. Phys. Chem. B 104 (12), 2759–2766.

Bard, A.J., Faulkner, L.R., 2001. Electrochemical Methods. Fundamental and Applications, second ed. J. Wiley & Sons, New York, Chichester, Brisbane, Toronto, Singapore, pp. 103–104.

Bond, D.R., Holmes, D.E., Tender, L.M., Lovley, D.R., 2002. Electrode-reducing microorganisms that harvest energy from marine sediments. Science 295 (5554), 483–485.

Bond, D.R., Lovley, D.R., 2003. Electricity production by Geobacter sulfurreducens attached to electrodes. Appl. Environ. Microbiol. 69 (3), 1548–1555.

Clark, R.C., Bowden, E.F., 1997. Voltammetric peak broadening for cytochrome c/alkanethiolate monolayer structures: dispersion of formal potentials. Langmuir 13 (3), 559–565.

Collinson, M., Bowden, E.F., Tarlov, M.J., 1992. Voltammetry of covalently immobilized cytochrome-c on self-assembled monolayer electrodes. Langmuir 8 (5), 1247–1250.

El Kasmi, A., Wallace, J.M., Bowden, E.F., Binet, S.M., Linderman, R.J., 1998. Controlling interfacial electron-transfer kinetics of cytochrome c with mixed self-assembled monolayers. J. Am. Chem. Soc. 120 (1), 225–226.

Fan, R., Chen, X.H., Gui, Z., Liu, L., Chen, Z.Y., 2001. A new simple hydrothermal preparation of nanocrystalline magnetite Fe_3O_4. Mater. Res. Bull. 36 (3–4), 497–502.

Froelich, P.N., Klinkhammer, G.P., Bender, M.L., Luedtke, N.A., Heath, G.R., Cullen, D., Dauphis, P., Hammond, D., Hartman, B., Maynard, V., 1979. Early oxidation of organic-matter in pelagic sediments of the eastern equatorial Atlantic—suboxic diagenesis. Geochim. Cosmochim. Acta 43 (7), 1075–1090.

Holmes, D.E., Bond, D.R., O'Neil, R.A., Reimers, C.E., Tender, L.M., Lovley, D.R., 2004a. Microbial communities associated with electrodes harvesting electricity from a variety of aquatic sediments. Microb. Ecol. 48 (2), 178–190.

Holmes, D.E., Bond, D.R., Lovley, D.R., 2004b. Electron transfer by *Desulfobulbus* propionicus to Fe(III) and graphite electrodes. Appl. Environ. Microbiol. 70 (2), 1234–1237.

Lovley, D.R., Coates, J.D., BluntHarris, E.L., Phillips, E.J.P., Woodward, J.C., 1996. Humic substances as electron acceptors for microbial respiration. Nature 382 (6590), 445–448.

Lovley, D.R., Holmes, D.E., Nevin, K.P., 2004. In: Poole, R.K. (Ed.), Advances in Microbial Physiology, vol. 49. Elsevier Academic, London, pp. 219–286.

Park, D.H., Zeikus, J.G., 2002. Impact of electrode composition on electricity generation in a single-compartment fuel cell using Shewanella putrefaciens. Appl. Microbiol. Biotechnol. 59 (1), 58–61.

Park, D.H., Zeikus, J.G., 2003. Improved fuel cell and electrode designs for producing electricity from microbial degradation. Biotechnol. Bioeng. 81 (3), 348–355.

Mahadevan, R., Bond, D.R., Butler, J.E., Esteve-Nuñez, A., Coppi, M.V., Palsson, B.O., Schilling, C.H., Lovley, D.R., 2006. Characterization of metabolism in the Fe(III)-reducing organism *Geobacter sulfurreducens* by constraint-based modeling. Appl. Environ. Microbiol. 72 (2), 1558–1568.

Reimers, C.E., Tender, L.M., 2002. Unpublished results.

Reimers, C.E., Tender, L.M., Fertig, S., Wang, W., 2001. Harvesting energy from the marine sediment-water interface. Environ. Sci. Technol. 35 (1), 192–195.

Reimers, C., Girguis, P., Westall, J., Newman, D., Stecher, H., Howell, K., Alleau, Y., 2005. Using electrochemical methods to study redox processes and harvest energy from marine sediments. In: Goldschmidt Conference Abstracts. Oxidation–reduction reactions in marine sediments, p. A575.

Ryckelynck, N., Stecher III, H.A., Reimers, C.E., 2005. Understanding the anodic mechanism of a seafloor fuel cell: interactions between geochemistry and microbial activity. Biogeochemistry. 76, 113–139.

Tarlov, M.J., Bowden, E.F., 1991. Electron-transfer reaction of cytochrome-c adsorbed on carboxylic-acid terminated alkanethiol monolayer electrodes. J. Am. Chem. Soc. 113 (5), 1847–1849.

Tender, L.M., Reimers, C.E., Stecher III, H.A., Holmes, D.E., Bond, D.R., Lowy, D.A., Pilobello, K., Fertig, S.J., Lovley, D.R., 2002. Harnessing microbially generated power on the seafloor. Nat. Biotechnol. 20 (8), 821–825.

Wilcock, W.S.D., Kauffman, P.C., 1997. Development of a seawater battery for deep-water applications. J. Power Sources 66 (1–2), 71–75.

Wu, Y.P., Jiang, C., Wan, C., Holze, R., 2002. Modified natural graphite as anode material for lithium ion batteries. J. Power Sources 111 (2), 329–334.